Full Paper

Propellants, Explosives, Pyrotechnics

DOI: 10.1002/prep.201400060

Molecular Origin of the Influence of the Temperature on the Loss Factor of a Solid Propellant

Aurélie Azoug,*[a] Robert Nevière,[b] and Andrei Constantinescu[a]

Abstract: This study focuses on the viscoelastic behavior of an industrial hydroxyl-terminated polybutadiene (HTPB) based solid propellant. The analysis of the loss factor as function of temperature enables the investigation of the molecular mechanisms participating in the nonlinear viscoelastic behavior. A design of experiments determines the influences of the filler fraction, of the NCO/OH ratio, of the plasticizer content, and of the presence or absence of filler-binder bonding agents. For all the tested materials, the loss factor as function of temperature exhibits two distinct peaks when measured by Dynamic Mechanical Analysis. Exponentially modified Gaussian distributions are applied on each peak to characterize the behavior. While the first peak is commonly associated with the rubber-glass transition of the material, the second peak has not been clearly associated with a molecular mechanism. This study shows that the second peak of the loss factor in HTPB-based solid propellants originates from the flow of free polymer chains in the polymer network with a reptation mechanism. The sol polymer fraction controls the area of the second peak, whereas its temperature at the maximum corresponds to an activation temperature determined by the molar masses of the sol polymer. Finally, when the propellant is stretched, a decrease in area and an increase in the temperature of the peak show that the reptation of the sol polymer chains is constrained by the network.

Keywords: Highly-filled elastomer · Solid propellant · Dynamic Mechanical Analysis (DMA) · Loss factor · Sol fraction

1 Introduction

Solid propellants are highly-filled elastomers used for propulsion of rockets and launchers. These materials exhibit a complex heterogeneous microstructure where the various components interact with each other. Highly-filled elastomers have a filler volume fraction of up to 80 %. As dewetting is the main damage mechanism in solid propellants, filler-binder bonding agents (FBBA) are added to the composition to promote the adhesion of binder polymer chains to the surfaces of the fillers.

A high quantity of plasticizers is introduced into the premix during manufacture. These molecules aim at facilitating the process, particularly the incorporation of fillers, and at providing targeted mechanical properties of the final product. Moreover, the hydroxyl-terminated polybutadiene (HTPB) polymer network of solid propellants is intentionally under cross-linked. Consequently, part of the polymer remains unlinked to the network. These free polymer chains are hereafter named sol polymer. We define the sol fraction as the microstructural phase that can be extracted by swelling, meaning this part of the binder is not linked to the network and does not contribute to the elastic response. The sol fraction in solid propellants is mainly constituted of plasticizer molecules and sol polymer chains.

The determination of structure-property relationships is made difficult by this complex microstructure. The viscoelastic behavior can be characterized by the complex modulus and the loss factor. We performed in previous publications a comprehensive study of the viscoelasticity of HTPB-based solid propellants at room temperature [1–5]. The presented study focuses on the influence of temperature on the viscoelasticity. Since the analysis of the complex modulus according to temperature does not provide more insight into the molecular mechanisms than the study already performed at room temperature [6], this paper will focus on the evolution of the loss factor with temperature.

The loss factor measured by Dynamic Mechanical Analysis (DMA) experiments corresponds to the damping ability of the material, i.e. its ability to dissipate energy. This factor strongly depends on the applied sinusoidal strain and on the temperature. In HTPB-based composite propellants, the loss factor evolution according to temperature presents two peaks [7], one situated between −90 °C and −50 °C and the other one at higher temperatures. The peak at lower temperatures is commonly associated with the glass

[a] *A. Azoug, A. Constantinescu*
Laboratoire de Mécanique des Solides
CNRS UMR 7649
Ecole Polytechnique
Palaiseau, France
**e-mail: aurelie.azoug@polytechnique.edu*

[b] *R. Nevière*
Herakles, Centre de Recherches du Bouchet
rue Lavoisier
Vert-le-Petit, France

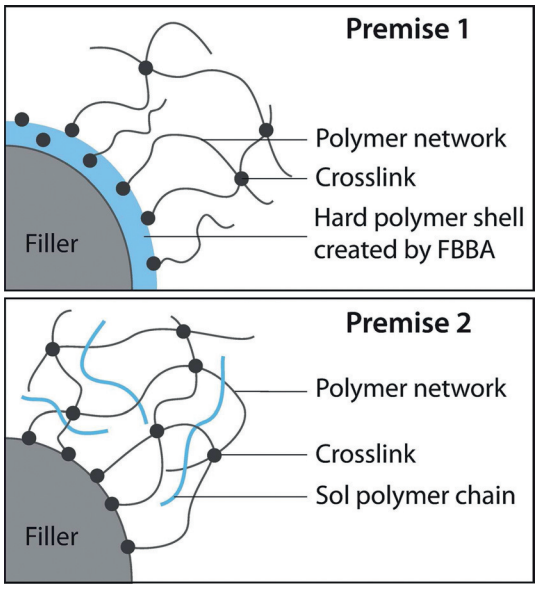

Scheme 1. Microstructure of the solid propellant according to each premise.

transition of the material [8], whereas the molecular origin of the second peak observed on the loss factor curve according to temperature is still an open question.

The following explanation has been suggested for the molecular mechanism leading to a second peak on the loss factor curve in solid propellants and more generally in filled elastomers. We refer to this explanation as Premise 1.

Premise 1: Two domains are physically separated in polyurethanes materials, i.e. rigid and soft phases corresponding to rigid segment agglomerates and soft segments. These materials present a two-peak loss factor, each peak corresponding to the glass transition of one domain [9–11]. This observation has been adapted to the case of filled elastomers and solid propellants by suggesting that a rigid layer of polymer at the binder-filler interphase constitute the hard phase (Scheme 1 Premise 1) [12,13]. The hard phase exhibits a rubber-glass transition at a higher temperature than the one of the rest of the binder [14–16]. Adopting this premise, the second peak originates from the glass transition of the hard phase.

A second explanation derives from physico-chemical studies of guest polymer chains into polymer networks. This premise has been proposed for unfilled and filled systems but has never been discussed in the case of solid propellants.

Premise 2: In the case of guest free polymer chains in a polybutadiene network, it has been proposed that the second peak of the loss factor corresponds to the flow of the free molecules (Scheme 1 Premise 2) [17,18]. The free chains move inside the network with a reptation mechanism [19], described by the molecular dynamic tube model [20,21].

An identical behavior has been observed for other networks containing free polymer chains in unfilled [22,23] and filled materials [24]. In addition, Nevière and Guyader [25] measured the loss factor of a cross-linked HTPB binder before and after extraction of the sol fraction. Because the loss factor second peak disappears after extraction, they link the phenomenon to the presence of the sol fraction rather than to a hard phase transition. However, they did not establish a precise mechanism. A similar study [26] attributed the decrease of the second peak area with aging to a decrease in molecular mobility.

This study aims at identifying, which molecular mechanism applies to solid propellants. Moreover, the influence of deformation on the determined molecular mechanism is analyzed.

2 Experimental Section

2.1 Materials

A comprehensive description of the optimal Design of Experiments (DoE) and the obtained materials has been provided in previous publications [1,2]. The main elements of the composition are given in the following. The DoE factors are the formulation ingredients most influential on the mechanical behavior. Four factors are chosen:

(i) the filler fraction: between 86 and 90 wt-%,

(ii) the NCO/OH ratio: between 0.8 and 1.1,

(iii) the plasticizer content: between 10 and 30 % mass of the binder,

(iv) the binder-filler bonding agents (FBBA): absent or present (categorical).

The fillers are ammonium perchlorate and aluminum particles. The exact synthesis of the FBBA molecules is not communicated due to confidentiality restrictions. Their mechanism is described in [1]. Briefly, the FBBA is a combination of two molecules, denoted X and Y hereafter.

Molecule X reacts with the curing agent and the filler surface and is introduced in each material, independently of the FBBA factor level. Hence, the influence of molecule X on the polymer network is the same for all the materials. Molecule Y contains aziridine groups that envelop the filler in a dense strengthening layer. Efficient adhesion is created when both molecules X and Y are introduced.

The chemical interactions between the compounds are complex and the exact mechanisms leading to proper filler-binder adhesion are difficult to quantify. Therefore, this factor is chosen to be categorical and presents two levels: absence (−) or presence (x) of molecule Y.

The binder is based on hydroxy-terminated polybutadiene (HTPB) prepolymer cured with a methylene bis(4-cyclohexylisocyanate) (HMDI). The prepolymer has a mean molar mass of 2900 g mol^{-1} and a mean functionality of 2.3. The ratio of the quantity of curing agents (NCO) with respect to the quantity of hydroxyl functions (OH) is the NCO/OH ratio [27]. This value measures the relative

Table 1. Materials manufactured after the DoE method. FBBA absence or presence is denoted by – and x, respectively.

Material	Fillers [mass %]	FBBA	NCO/OH ratio	Plasticizer [% mass binder]	Sol fraction [% mass polymer]	$T_{g,DSC}$ [°C]
0	86	–	1.1	10	16.67	−76.2
1	90	–	0.8	30	90.00	−82.0
2	86	x	1.1	20	5.36	−78.5
3	90	x	0.8	20	57.50	−80.9
4	86	–	1.1	30	6.12	−80.9
5	90	x	1.1	30	7.14	−82.2
6	90	–	0.8	10	48.89	−77.3
7	86	x	0.8	10	42.06	−77.0
8	86	–	0.8	20	54.46	−81.4
9	86	x	0.8	30	60.20	−81.9
10	90	–	0.95	20	31.25	−77.8
11	88	–	1.1	20	16.67	−81.4
12	90	x	1.1	10	13.33	−75.5
13	88	x	0.95	30	19.05	−81.4
14	88	x	0.95	15	20.59	−78.7
15	88	–	0.88	25	38.89	−81.9
16	88	–	0.95	10	25.93	−77.1
17	90	x	0.8	10	52.22	−76.0
18	86	–	0.8	10	50.79	−76.5
19	86	x	1.1	10	8.73	−79.1
20	89	–	1.1	20	14.77	−77.9
21	89	–	0.8	10	51.52	−77.2

amount of curing agents available to form a polymer network. At values lower than 1, a part of the prepolymer is not linked to the global network and is therefore extractable. As a consequence, it constitutes a part of the sol fraction and is named sol polymer.

The introduced plasticizer is dioctyl azelate (DOZ). A plasticizer content of at least 10% mass of the binder is necessary to manufacture the material. The molecules of plasticizer do not bind with the network or the fillers and are located only in the sol fraction [28].

The materials are thermally cured for two weeks at 50 °C. The levels of the factors for each of the 22 manufactured materials are given in Table 1.

2.2 Differential Scanning Calorimetry (DSC)

The glass transition temperature $T_{g,DSC}$ was determined by Differential Scanning Calorimetry (DSC) with a Mettler Toledo DSC 30 apparatus. One sample for each material was submitted to two cycles of temperature, cooling from 20 °C to −120 °C at a cooling rate of −20 °C min^{-1} and heating from −120 °C to 100 °C at a heating rate of 5 °C min^{-1}. The measurement takes place in a nitrogen atmosphere (40 mL min^{-1}). The $T_{g,DSC}$ values are the mean values of the inflection points in the heating phase of both cycles.

2.3 Swelling Experiments

The swelling experiments follow the swelling to equilibrium procedure described in details in Ref. [1]. To summarize, three specimens for each material were tested. The initial mass of the specimens is m_0. The specimens were placed in a toluene bath until swelling equilibrium was reached, usually four to five days. The solvent was evaporated until a constant dry mass m_{dp} was reached. Mass loss M_{sf} after extraction and drying indicates the mass of sol fraction in the initial formulation: $M_{sf}=m_0-m_{dp}$. The sol fraction in propellants is mainly constituted of polymer chains and plasticizer molecules. In the sequel, we shall denote by M_{solpol} and V_{solpol} the mass and volume of polymer chains in the sol fraction, and by M_{plast} and V_{plast} the mass and volume of plasticizer molecules. M_{plast} corresponds to the mass of plasticizers introduced during the manufacturing of the material (Table 1). If some additives are extracted, their mass is assumed to be insignificant. M_{solpol} is then deduced by $M_{solpol}=M_{sf}-M_{plast}$. The volume of the sol fraction, V_{sf}, and of its components are determined using the density of the polymer and the plasticizer, $\rho_{pol}=910\ \mathrm{kg\,m^3}$ and $\rho_{plast}=920\ \mathrm{kg\,m^3}$, respectively.

$$V_{sf} = V_{solpol} + V_{plast} = \frac{M_{solpol}}{\rho_{pol}} + \frac{M_{plast}}{\rho_{plast}}.$$

Finally, the fraction of sol polymer, F_{solpol}, is determined through:,

$$F_{solpol} = \frac{V_{solpol}}{V_{pol}} = \frac{V_{sf}-V_{plast}}{V_{pol}},$$

where the polymer volume fraction in the binder is assumed to be $V_{pol}=V_{binder}-V_{plast}$.

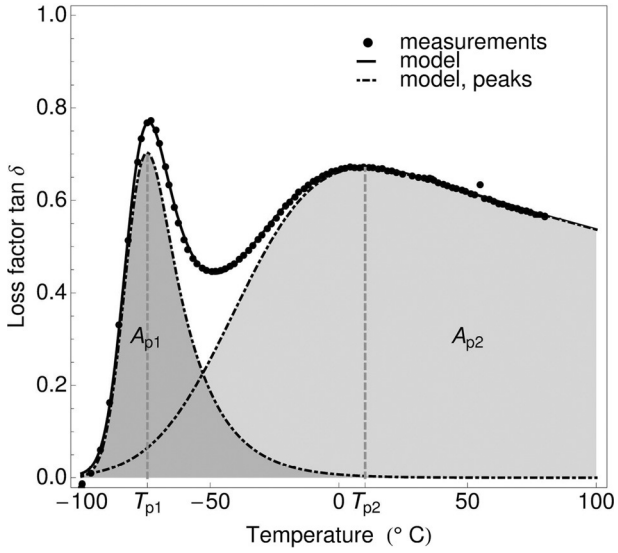

Figure 1. Example of loss factor measurements evaluation (material 1, $\varepsilon_0 = 0\,\%$).

2.4 Dynamic Mechanical Analysis

Prestrained Dynamic Mechanical Analysis experiments were achieved with a Metravib Viscoanalyseur VA3000. Rectangular specimens of dimension $25 \times 10 \times 5$ mm^3 were placed in the oven of the DMA apparatus. The temperature was raised to 80 °C and maintained for 15 min to allow temperature stabilization into the sample. The temperature then linearly decreased from 80 °C to −100 °C at a rate of $-2\,^{\circ}\mathrm{C\,min^{-1}}$. For each measurement at a given temperature, a sinusoidal strain of amplitude ε_a was superimposed to a prestrain ε_0. The total strain is

$$\varepsilon(t) = \varepsilon_0 + \varepsilon_a \sin(2\pi f t),$$

where $\varepsilon_a = 0.04\,\%$, and $f = 7.8$ Hz. Two prestrain values were tested, $\varepsilon_0 = 0\,\%$ and $\varepsilon_0 = 2\,\%$. According to the previous studies at room temperature [1,2], these values correspond to the linear and nonlinear domain, respectively. A new sample was used for each prestrain value.

The norm of the complex modulus $||E^*||$ and the loss factor $\tan\delta$ are determined at each temperature and prestrain level. The evolution of the storage and loss moduli with temperature did not provide any significant insight compared to studies at room temperature. Consequently, the study focuses on the analysis of the loss factor evolution with temperature, considering the influence of prestrain and propellant composition.

The curve of $\tan\delta$ exhibits two peaks (Figure 1). An exponentially modified Gaussian (EMG) distribution [Equation (1)] is fitted on each peak, following the method suggested by [14]. This function corresponds to a Gaussian distribution asymmetrically modified by an exponential. EMG functions are commonly used to fit chromatographic peaks [29,30].

$$EMG_i(T) = \frac{A_{pi}}{2k_i}\, exp\left[\frac{1}{2}\left(\frac{w_i}{k_i}\right)^2 - \frac{T - T_{ci}}{k_i}\right] * \left[1 + erf\left(\frac{T - T_{ci}}{\sqrt{2}w_i} - \frac{w_i}{\sqrt{2}k_i}\right)\right]$$

where T is the temperature, A_{pi} is the area of the peak, T_C is the temperature at the maximum of the Gaussian part, w is the half width at half height of the Gaussian part, k is the modification factor (skewness) introduced by the exponential, and $i = 1,2$ is the peak number (Figure 1). The optimization of the parameters of both $EMG_i(T)$ is done in two steps using a least-square algorithm in Mathematica®. First, data corresponding to the first peak at $T < -50^{\circ}$ are selected and the distribution $EMG_1(T)$ is fitted. Then, the obtained values (h_1, w_1, τ_1, T_{p1}) are indicated as initial values for the fitting of $EMG_1(T) + EMG_2(T)$ on the curve for the whole temperature range. Figure 1 shows an example of experimental measurements, fitted two peaks and their sum, constituting the model.

Since at elevated temperatures the loss factor spectrum does not decrease to a plateau value, the data treatment could require a baseline. In order to define a baseline, it would have been necessary to measure the behavior of all 22 materials up to the temperature, at which the second peak is complete for all of them. Because propellants are energetic materials, this could not be achieved without a serious breach of safety. As a consequence, we chose not to determine a baseline but instead to identify the $EMG_2(T)$ function of the second peak as it was measured. The advantage of the DoE is that, even though an error is made systematically on the processing of the data, the comparison of the behavior of the materials is statistically valid. The influence of the composition on the second peak of the loss factor is determined with this method but neither quantification nor activation energy will be suggested for the phenomenon leading to the second peak of the loss factor.

Two parameters are defined for each EMG peak, which allows comparing the results obtained for all materials of the DoE. These parameters are the temperature of the maximum T_{pi} and the area A_{pi}, of the peak EMG_i, where i is the peak number (Figure 1). They constitute the response of the DoE. More precisely, for the second peak, the response studied is $T_{p2} - T_{g,DSC}$ since the glass transition temperature is considered an intrinsic temperature property for each material. The glass transition temperature measured by DSC experiments was chosen as the temperature reference. As the first peak of the loss factor is commonly associated with the glass transition [8], the response T_{p1} is sometimes used as a measure of $T_{g,DMA}$. For this reason, T_{p1} is not modified but compared with $T_{g,DSC}$.

Finally, the same procedure is used on the experimental measurements with prestrain $\varepsilon_0 = 2\,\%$ and the variation of T_{p2} and A_{p2} according to prestrain is also treated as a re-

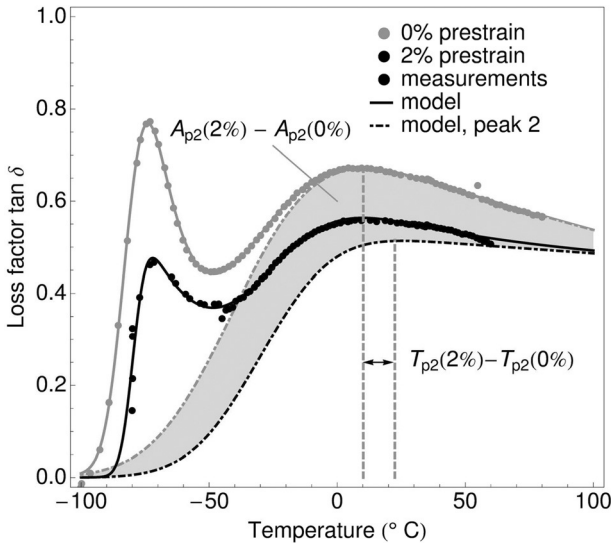

Figure 2. Parameters showing the influence of prestrain on tanδ second peak (material 1).

sponse of the DoE (Figure 2). The variation of T_{p1} was not significant enough to be studied with this method. Finally, the processing of the variation of A_{p1} was deemed impossible since the results showed that A_{p1} does not depend on the factors of the DoE (see Results and Discussion Section 3.2).

2.5 DoE Analysis

Finally, as presented in detail in the literature [1,2], the DoE method was applied to the six chosen responses of the DoE, which are T_{p1}, A_{p1}, $T_{p2}-T_{g,DSC}$, A_{p2}, $T_{p2}(2\%)-T_{p2}(0\%)$, $A_{p2}(2\%)-A_{p2}(0\%)$ using the Design-Expert® software [31].

A model with n coefficients can only be investigated with a DoE consisting of at least n runs. According to the number of factors chosen and the number of materials manufactured, the possible models are: mean value, linear, first order interactions, or quadratic. The unknown constants of the model are obtained by optimization on the experimental results. An analysis of variance determines the model form best representing the results while taking into account the least number of terms. A second analysis of variance is performed on the chosen model form to eliminate the terms corresponding to non-influential factors or interactions (p value < 0.05).

The final model represents the response according to the factors of the DoE, herein variables of material composition. The good fit of the model was evaluated by the adjusted correlation coefficient $R^2_{adjusted}$ [32], which takes into account the number of parameters in the model.

3 Results and Discussion

The values of the responses of the DoE for each material are compiled in Table 2.

3.1 Glass Transition and Loss Factor of the First Peak

The adjusted correlation coefficients $R^2_{adjusted}$ of T_{p1} and A_{p1} are 0.88 and 0.26, respectively. It appears that the model obtained for A_{p1} is not statistically representative for the experimental values. Hence, this coefficient will not be ana-

Table 2. Results of the evaluation of the loss factor curves for each material.

Material	T_{p1} [°C]	A_{p1} [°C]	$T_{p2}-T_{g,DSC}$ [°C]	A_{p2} [°C]	$T_{p2}(2\%)-T_{p2}(0\%)$ [°C]	$A_{p2}(2\%)-A_{p2}(0\%)$ [°C]
0	−67.86	17.84	79.28	29.41	0.23	2.37
1	−74.51	20.76	92.12	90.86	15.41	−24.46
2	−70.80	18.53	85.54	31.09	4.24	2.83
3	−71.08	14.33	103.08	92.05	−26.18	−21.62
4	−73.88	14.80	83.72	37.63	11.87	−0.16
5	−71.63	18.30	78.93	38.65	12.30	−3.57
6	−69.49	18.66	96.69	57.95	16.28	−2.14
7	−69.96	18.81	101.90	64.93	7.49	−10.12
8	−71.85	21.91	94.76	86.55	8.20	−8.52
9	−75.44	21.37	90.61	87.98	20.80	3.57
10	−71.17	19.77	80.23	48.94	11.91	−9.48
11	−71.18	19.87	83.93	27.76	2.00	1.13
12	−66.71	16.46	84.62	32.83	18.02	−2.90
13	−73.90	19.20	90.63	48.84	9.88	−5.42
14	−71.52	17.53	92.43	39.64	15.41	−2.83
15	−71.56	20.19	93.83	62.09	1.57	−8.30
16	−68.19	19.39	86.56	33.52	7.10	1.67
17	−69.28	20.04	93.89	69.38	18.61	−11.43
18	−69.53	18.14	93.30	74.63	6.95	−7.73
19	−69.53	17.25	87.08	27.18	11.27	−0.51
20	−69.19	12.51	71.51	37.53	10.71	−7.67
21	−69.27	20.61	95.54	60.81	6.47	−2.47

lyzed. This lack of correlation shows that the area of the first peak is not the direct result of the chosen factors for the composition of the material.

However, the adjusted correlation coefficient for T_{p1} is satisfying and the model states the influences of filler fraction, NCO/OH ratio and plasticizer content on T_{p1} (Figure 3). The plasticizer content is the most significant controlling factor.

The temperature T_{p1} is related to the glass transition temperature $T_{g,DSC}$ [8], i.e. to the segmental mobility of the polymer chains in the binder, and this observation is verified in this system (Figure 4).

Moreover, the influence of plasticizer content on T_{p1} is similar to the one obtained for $T_{g,DSC}$. A line is optimized by a least-square minimization in Mathematica®. Its slope is 1, however temperatures T_{p1} are on average superior to the corresponding $T_{g,DSC}$ by 8.2 °C. This discrepancy is the result of the mechanical character of the DMA measurement.

The DSC scan shows only one transition at the temperature identified as $T_{g,DSC}$. Taking into account the difference in values due to the difference in measurement methods, the glass transition of the complete material seems to correspond to the temperature of the first peak of the loss factor for all the materials. That observation challenges Premise 1, as several studies on polymer systems showing two glass transitions confirm this explanation with changes in the heat capacity of the material at distinct temperatures [10, 11].

3.2 Molecular Origin of the Loss Factor Second Peak

The adjusted correlation coefficients for $T_{p2}-T_{g,DSC}$ and A_{p2} are 0.73 and 0.97, respectively. The filler fraction has no influence on $T_{p2}-T_{g,DSC}$ (Figure 5). The effect of the filler fraction on A_{p2} depends on FBBA presence and is extremely small.

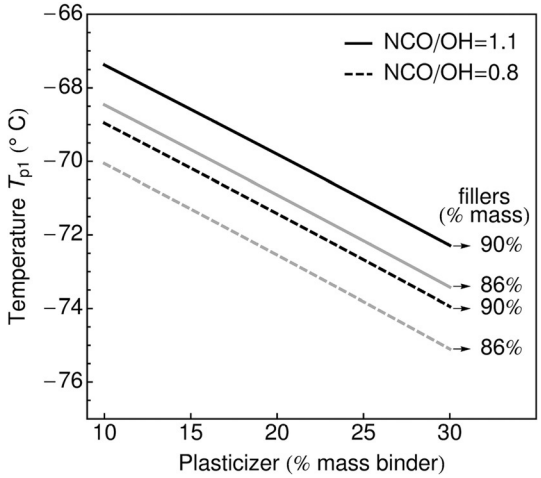

Figure 3. Influence of filler fraction, NCO/OH ratio, and plasticizer content on T_{p1}. T_{p1} increases with filler fraction and NCO/OH ratio, and decreases with an increase in plasticizer content.

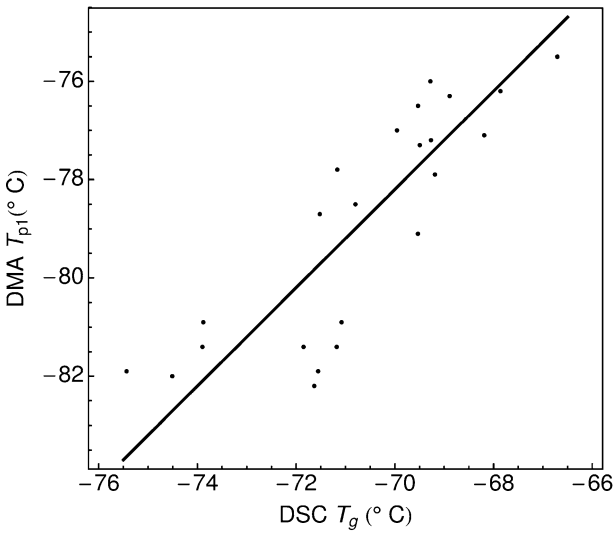

Figure 4. Comparison of T_g measured by DSC and T_{p1} measured by DMA. A correlation is found between $T_{g,DSC}$ and $T_{g,DMA}$.

Premise 1 states that the loss factor second peak could be the expression of the glass transition of a harder phase in the microstructure. The ammonium perchlorate fillers introduced in propellants are not active fillers. As a consequence, their surface does not attract polymer chains by absorption, as would carbon black or silica fillers. Only when FBBA is added are the binder-filler chemical links promoted and the presence of a hard layer is possible. In some cases, the layer of more rigid polymer created by FBBA around the fillers is assumed to constitute the hard phase. Since the area of the peak does not significantly evolve with the filler fraction or the presence of FBBA, Premise 1 does not justify the results obtained here. The

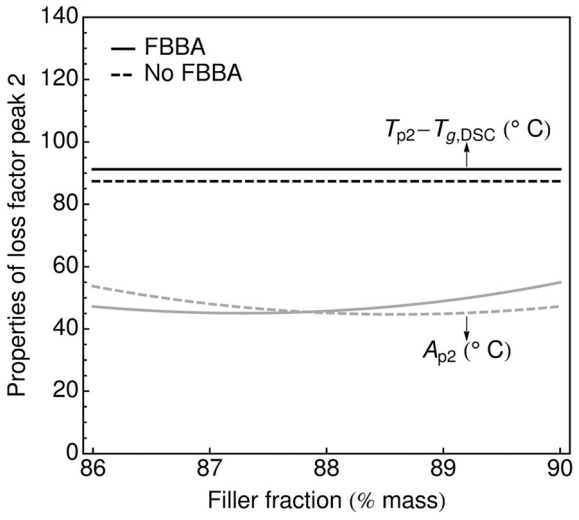

Figure 5. Influence of filler fraction on $T_{p2}-T_{g,DSC}$ and A_{p2}. (NCO/OH = 0.95, plasticizer = 20% mass of the binder). The filler fraction has no influence on $T_{p2}-T_{g,DSC}$, and its effect on A_{p2}. is extremely small.

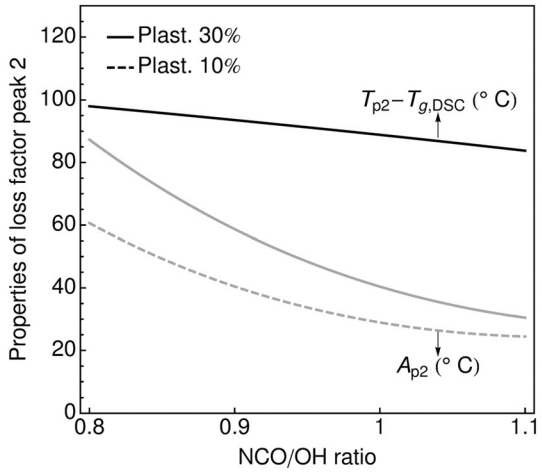

Figure 6. Influence of NCO/OH ratio and plasticizer content on $T_{p2}-T_{g,DSC}$ and A_{p2} (filler fraction = 88 % mass, FBBA present, plasticizer in % mass of the binder). The area A_{p2} decreases with an increase of the NCO/OH ratio and increases with the plasticizer content. $T_{p2}-T_{g,DSC}$ decreases as the NCO/OH ratio increases. The plasticizer content has no influence on $T_{p2}-T_{g,DSC}$.

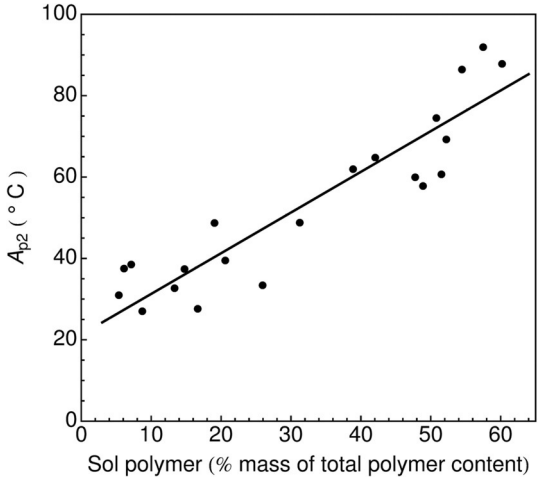

Figure 7. Correlation between A_{p2} and sol polymer quantity. Sol polymer fraction determined by swelling experiments [1,2]. A direct relationship between A_{p2} and the sol polymer fraction is shown for all 22 materials independently of the levels of filler fraction, NCO/OH ratio, and plasticizer content, and of the presence of FBBA.

limited influence of the filler fraction on the second peak of the loss factor indicates that the studied phenomenon takes place in the bulk of the binder rather than around the fillers. Consequently, Premise 1 does not account for the experimental results obtained for these solid propellants.

The influence of FBBA on the results is linked to their influence on the microstructure. We previously showed that FBBA molecules react with curing agents to form binder-filler links [1]. This reaction deprives the network of necessary curing agents and, hence, indirectly increases the amount of sol polymer in the sol fraction. Further analysis of the results will provide evidence of the role of this sol fraction in the relaxation mechanism.

Let us further consider the possibility that Premise 2 would explain this behavior. The area A_{p2} decreases with an increase of the NCO/OH ratio and increases with the plasticizer content (Figure 6).

A previous article [2] established that the sol polymer quantity decreases when the NCO/OH ratio increases and increases with plasticizer content as long as the NCO/OH ratio is below the stoichiometric ratio. However, the influence of the plasticizer content on the sol polymer fraction is not as significant as the influence of the NCO/OH ratio.

Figure 6 shows that the influences of the NCO/OH ratio and the plasticizer content on A_{p2} exhibit the same tendencies as their influence on the sol polymer fraction. The direct relationship between A_{p2} and the sol polymer fraction is further confirmed by Figure 7, where a clear correlation is shown for all 22 materials independently of the levels of filler fraction, NCO/OH ratio, and plasticizer content, and of the presence of FBBA.

Though A_{p2} seems to be proportional to the sol polymer quantity, this value also takes into account the contribution of the polymer network because no baseline was defined. It has been determined in a similar study on an unfilled material that this contribution is less than one order of magnitude compared to the contribution of sol polymer chains and hence can be neglected [23]. Although the polymer system studied in [23] was different, we assume that the contribution of the polymer network in solid propellants is small enough to be neglected here.

Consequently, A_{p2} is representative of the quantity of sol polymer chains in the microstructure and Premise 2 properly explains the behavior of this system. The second peak of the loss factor curve originates from a molecular relaxation of the free polymer molecules in the polymer network.

$T_{p2}-T_{g,DSC}$ decreases as the NCO/OH ratio increases. The plasticizer content has no influence on $T_{p2}-T_{g,DSC}$ (Figure 6).

Gel permeation chromatography measurements of the polymer chains in the sol polymer fraction showed that the molar masses of the sol polymer chains increase with an increase of the sol polymer fraction. Since the molar masses of the sol polymer chains were measured only for few materials of the design of experiments, the influences of the NCO/OH ratio and of the plasticizer content on this quantity cannot be rigorously determined. However, the strong increases in sol polymer fraction as well as in the molar masses in this sol fraction with a decrease of the NCO/OH ratio lead us to assume that $T_{p2}-T_{g,DSC}$ is governed by the molar mass of the sol polymer chains (Figure 8).

Identically, Sidorovich et al. [17] showed for mixtures of a polybutadiene network and rubbers of different molecular masses that the diminution of the molar masses of the sol polymer chains results in a decrease of T_{p2}.

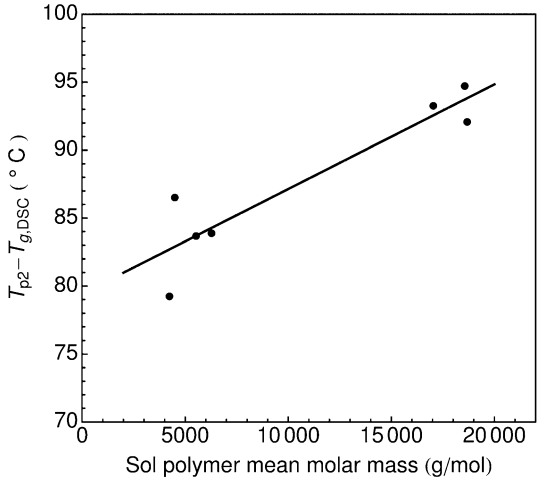

Figure 8. Correlation between T_{p2} and sol polymer mean molar mass for materials 0, 1, 4, 8, 11, 16, and 18. Mean molar masses determined by gel permeation chromatography [1,2]. $T_{p2}-T_{g,DSC}$ is governed by the molar mass of the sol polymer chains.

As a conclusion, Premise 2 fully describes the obtained results characterizing the second peak of the loss factor. The relaxation mechanism leading to the second peak depends on the molecular mobility of the sol polymer chains in the network. It should be noted here that we differentiate the molecular mobility, defined as the ability of the molecule to move as a whole, from the segmental mobility, defined at a lower scale as the ability of the segments to move with respect to each other to allow the chain to reach a new configuration. The restriction of the segmental mobility corresponds to the glass transition, whereas the restriction of molecular mobility corresponds to a change in the second peak relaxation. The molecular mobility of these chains corresponds to their ability to flow in the network. More precisely, the second peak of the loss factor is due to the flow of sol polymer chains in the network using a reptation mechanism. The molar mass of the sol polymer chains controls the temperature of the peak, i.e. the temperature, at which the flow is activated, while the quantity of sol polymer defines the area of the peak.

3.3 Influence of Deformation

The evolution of T_{p2} and A_{p2} with prestrain is measured and processed in the framework of the DoE. The obtained models for $T_{p2}(2\%)-T_{p2}(0\%)$ and $A_{p2}(2\%)-A_{p2}(0\%)$ present adjusted correlation coefficients equal to 0.30 and 0.84 respectively. Consequently, the analysis of T_{p2} variation according to prestrain is limited. This limitation results from the addition of experimental and fitting errors in the measurement and identification of $T_{p2}(2\%)$ and $T_{p2}(0\%)$. Only the global trend, i.e. the sign of $T_{p2}(2\%)-T_{p2}(0\%)$, is discussed.

As the material is submitted to a prestrain, T_{p2} increases ($T_{p2}(2\%)-T_{p2}(0\%)>0$) regardless of the level chosen for the DoE factors and A_{p2} decreases ($A_{p2}(2\%)-A_{p2}(0\%)<0$) for almost all of the materials (Figure 9 and Figure 10). In addition, $A_{p2}(2\%)-A_{p2}(0\%)$ decreases as the filler fraction increases (Figure 9) and tends to zero as NCO/OH ratio increases (Figure 10).

For a small part of the tested domain, the change in A_{p2} is modeled as positive or close to 0 when the NCO/OH ratio is higher than 1. Considering the mechanism established in the first part of the discussion, the second peak depends on the sol polymer fraction. The lack of influence of the prestrain on A_{p2} for a high NCO/OH ratio is the consequence of the limited amount of sol polymer chains in

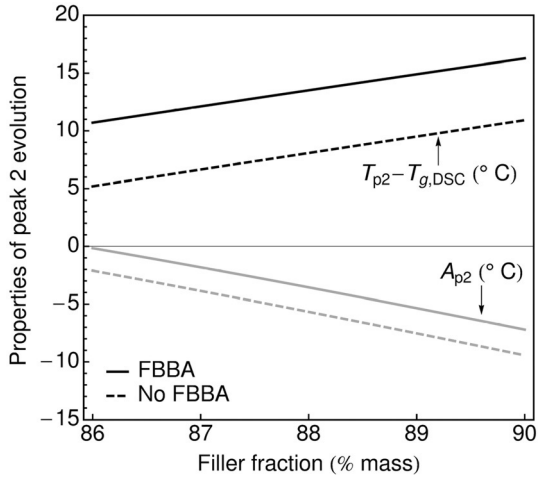

Figure 9. Influence of filler fraction on $T_{p2}(2\%)-T_{p2}(0\%)$ and $A_{p2}(2\%)-A_{p2}(0\%)$, (NCO/OH = 0.95, plasticizer = 20% mass of the binder). As the material is submitted to a prestrain, (T_{p2} increases $T_{p2}(2\%)-T_{p2}(0\%)>0$) regardless of the level chosen for the DoE factors and A_{p2} decreases ($A_{p2}(2\%)-A_{p2}(0\%)<0$) for almost all of the materials. $A_{p2}(2\%)-A_{p2}(0\%)$ decreases as the filler fraction increases.

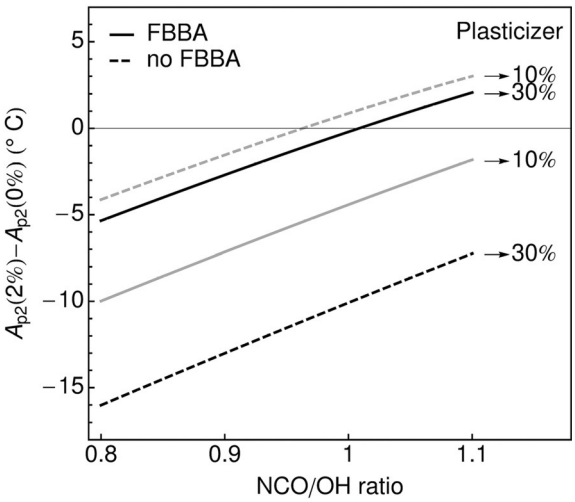

Figure 10. Influence of NCO/OH ratio, plasticizer content, and presence of FBBA, on $A_{p2}(2\%)-A_{p2}(0\%)$ (filler fraction = 88% mass, plasticizer in % mass of the binder). $A_{p2}(2\%)-A_{p2}(0\%)$ increases and tends to zero as NCO/OH ratio increases.

the material in the first place. As discussed in Section 3.2, A_{p2} decreases when NCO/OH ratio increases. Only a small fraction of the polymer chains flow with a reptation mechanism at 0% of prestrain. The influence of the prestrain is then insignificant.

The influences of the filler fraction and the FBBA are the direct result of strain amplification [1]. Because the propellants exhibit a high filler fraction (between 86 and 90% mass), the polymer network and sol polymer chains are highly constrained between the fillers and strain amplification effects are dominant.

Applying a prestrain causes part of the network reaching its maximal extensibility. As the network is stretched, the mesh size decreases and the flow of sol polymer chains occurs in a constrained way. In conformity with the tube model, if the mesh size diminishes, the reptation time is longer and the activation temperature higher. T_{p2} measures a mean temperature of activation for a relaxation phenomenon that occurs over a wide range of temperatures depending on the distribution of molar masses in the sol polymer fraction. The increase of T_{p2} with prestrain directly results from the deformation of the network.

The decrease in A_{p2} with an increasing prestrain means that the quantity of polymer chains able to flow into the network decreases.

When the NCO/OH ratio is sufficiently lower than the stoichiometric conditions, the effect of prestrain on A_{p2} is significant. As the prestrain is applied, a high quantity of sol polymer chains is constrained into the network and/or between the fillers. The molecular mobility of the sol polymer chains is then significantly restricted. As a consequence, the quantity of sol polymer chains that flow decreases.

As the plasticizer content increases, $A_{p2}(2\%)-A_{p2}(0\%)$ increases when FBBA are introduced and decreases when no FBBA are added (Figure 11). The strong interaction between plasticizer content and the FBBA-filler system has been analyzed previously [2] and will not be discussed further here. The results are severely biased by this interaction. On one hand, the role of plasticizer is to decrease intermolecular frictions and, as such, to promote molecular mobility. The observed increase of $A_{p2}(2\%)-A_{p2}(0\%)$ with plasticizer content could be the result of the actual plasticizing of the microstructure which would prevent the sol polymer chains to be blocked into the network. On the other hand, the large decrease of $A_{p2}(2\%)-A_{p2}(0\%)$ with plasticizer content when no FBBA are added is still an open question. One possible explanation is that the movements of the network around the fillers constitute the main dissipating mechanism preventing the thermal activation of the reptation of the sol polymer chains.

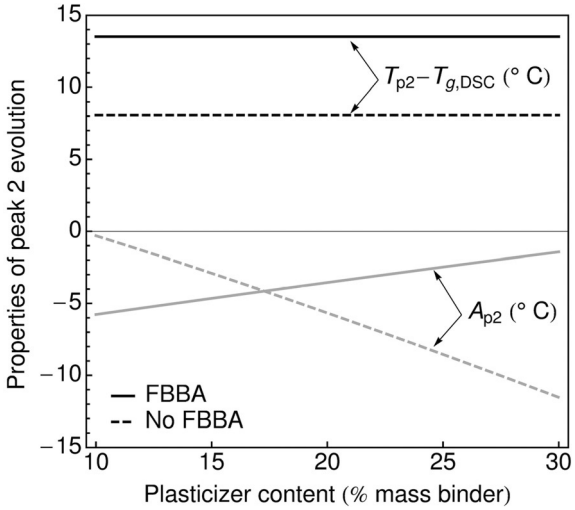

Figure 11. Influence of plasticizer content on $T_{p2}(2\%)-T_{p2}(0\%)$ and $A_{p2}(2\%)-A_{p2}(0\%)$, (filler fraction = 88% mass, NCO/OH = 0.95). As the plasticizer content increases, $A_{p2}(2\%)-A_{p2}(0\%)$ increases when FBBA are introduced and decreases when no FBBA are added.

4 Conclusions

This study focuses on the influence of temperature on the loss factor of HTPB-based solid propellants according to their composition. The implemented design of experiments determines the influence of the filler fraction, of the NCO/OH ratio, of the plasticizer content, and of the presence or absence of FBBA. The loss factor is measured by Dynamic Mechanical Analysis and exhibits two peaks in distinct temperature ranges. The two peaks are identified using exponentially modified Gaussian distributions.

The first peak of the loss factor corresponds to the rubber-glass transition of the material. The rubber-glass transition is defined by the modification of the segmental mobility of the polymer chains. This work shows that the second peak of the loss factor is associated to the molecular mobility of the sol polymer chains, i.e. the polymer chains extractable by swelling and as such not linked to the network. More precisely, the second peak corresponds to the flow of these sol polymer chains in the polymer network. The sol polymer fraction controls the area of the peak and the molar masses of the sol polymer chains control the activation temperature of the relaxation. Once the relaxation is thermally activated, the sol polymer chains flow in the network with a reptation mechanism. Finally, when a prestrain is applied to the propellant, a decrease in area and an increase in the activation temperature show that the reptation of the sol polymer chains is constrained by the network.

Acknowledgments

The work of A. A. is financially supported by DGA, Délégation Générale pour l'Armement (France). The authors would like to thank Mrs. Amiet (DGA) for supporting this project. The authors also thank the formulation department of Herakles-CRB for carefully manufacturing all the materials.

References

[1] A. Azoug, R. Nevière, R. M. Pradeilles-Duval, A. Constantinescu, Influence of the Fillers and the Bonding Agents on the Viscoelasticity of Highly-Filled Elastomers, *J. Appl. Polym. Sci.* **2014**, *131*, 40664.

[2] A. Azoug, R. Nevière, R. M. Pradeilles-Duval, A. Constantinescu. Influence of Crosslinking and Plasticizing on the Viscoelasticity of Highly-Filled Elastomers, *J. Appl. Polym. Sci.* **2014**, *131*, 40392.

[3] A. Thorin, A. Azoug, A. Constantinescu, Influence of Prestrain on Mechanical Properties of Highly-Filled Elastomers: Measurements and Modeling, *Polym. Test.* **2012**, *31*, 978–986.

[4] A. Azoug, A. Constantinescu, R. M. Pradeilles-Duval, M. F. Vallat, R. Nevière, B. Haidar, Effect of the Sol Fraction and Hydrostatic Deformation on the Viscoelastic Behavior of Prestrained Highly-Filled Elastomers, *J. Appl. Polym. Sci.* **2013**, *127*, 1772–1780.

[5] A. Azoug, A. Thorin, R. Nevière, R. M. Pradeilles-Duval, A. Constantinescu, Influence of Orthogonal Prestrain on the Viscoelastic Behavior of Highly-Filled Elastomers, *Polym. Test.* **2013**, *32*, 375 – 384.

[6] A. Azoug, *Micromécanismes et Comportement Macroscopique d'un Elastomère Fortement Chargé*, Ph. D. Thesis, Ecole Polytechnique, **2011**.

[7] A. Adicoff, A. H. Lepie, Effect of Tensile Strain on the Use of the WLF Equation, *J. Appl. Polym. Sci.* **1970**, *14*, 953–966.

[8] J. D. Ferry, *Viscoelastic Properties of Polymers*, 3rd ed., Wiley, New York, **1980**.

[9] J. L. de la Fuente, M. Fernández García, M. L. Cerrada, Viscoelastic Behavior in a Hhydroxyl-Terminated Polybutadiene Gum and its Highly Filled Composites: Effect of the Type of Filler on the Relaxation Processes, *J. Appl. Polym. Sci.* **2003**, *88*, 1705–1712.

[10] C. M. Brunette, S. L. Hsu, W. J. Macknight, N. S. Schneider, Structural and Mechanical Properties of Polybutadiene-Containing Polyurethanes, *Polym. Eng. Sci.* **1981**, *21*, 163 – 171.

[11] C. M. Brunette, W. J. Macknight, Thermal Transition and Relaxation Behavior of Polybutadiene Polyurethanes Based on 2,6-Toluene Diisocyanate, *Rubber Chem. Technol.* **1982**, *55*, 1413–1425.

[12] N. K. Dutta, D. Khastgir, D. K. Tripathy, The Effect of Carbon Black Concentration on the Dynamic Mechanical Properties of Bromobutyl Rubber, *J. Mater. Sci.* **1991**, *26*, 177 – 188.

[13] N. K. Dutta, D. K. Tripathy, Effects of Types of Fillers on the Molecular Relaxation Characteristics, Dynamic Mechanical, and Physical Properties of Rubber Vulcanizates, *J. Appl. Polym. Sci.* **1992**, *44*, 1635–1648.

[14] G. Tsagaropoulos, A. Eisenberg, Dynamic Mechanical Study of the Factors Affecting the Two Glass Transition Behavior of Filled Polymers. Similarities and Differences with Random Ionomers, *Macromolecules* **1995**, *28*, 6067 – 6077.

[15] S. Cerri, M. A. Bohn, Ageing Behaviour of Rocket Propellant Formulations with ADN as Oxidizer Investigated by DMA, DSC and SEM, *42nd Int. Annual Conference of ICT*, Karlsruhe, Germany, June 28–July 1, **2011**, p. 10.

[16] M. A. Bohn, G. Mußbach, S. Cerri, Influences on the Loss Factor of Elastomer Binders and its Modeling, *43rd Int. Annual Conference of ICT*, Karlsruhe, Germany, June 26–29, **2012**, p. 60.

[17] E. A. Sidorovich, A. I. Marei, N. S. Gashtol'd. High Temperature Relaxation Transitions in Elastomers, *Rubber Chem. Technol.* **1971**, *44*, 166 – 174.

[18] C. G. Robertson, C. M. Roland, Glass Transition and Interfacial Segmental Dynamics in Polymer-Particle Composites, *Rubber Chem. Technol.* **2008**, *81*, 506 – 522.

[19] O. Kramer, R. Greco, R. A. Neira, J. D. Ferry, Rubber Networks Containing Unattached Macromolecules. I. Linear Viscoelastic Properties of the System Butyl Rubber-Polyisobutylene, *J. Polym. Sci. Polym. Phys. Ed.* **1974**, *12*, 2361 – 2374.

[20] P. de Gennes, *Scaling Concepts in Polymer Physics*, Cornell University Press, Ithaca, **1979**.

[21] M. Doi, S. Edwards, *The Theory of Polymer Dynamics*, Clarendon Press, Oxford, **1986**.

[22] S. Ndoni, A. Vorup, O. Kramer, Random Polybutadiene Rubber Networks with Unattached Chains, *Macromolecules* **1998**, *31*, 3353 – 3360.

[23] K. Urayama, K. Yokoyama, S. Kohjiya, Visco-Elastic Relaxation of Guest Linear Poly(dimethyl-siloxane) in End-Linked Poly(dimethylsiloxane) Networks, *Macromolecules* **2001**, *34*, 4513 – 4518.

[24] A.-J. Zhu, S. S. Sternstein, Nonlinear Viscoelasticity of Nanofilled Polymers: Interfaces, Chain Statistics and Properties Recovery Kinetics, *Compos. Sci. Technol.* **2003**, *63*, 1113–1126.

[25] R. Nevière, M. Guyader, DMA : a Powerful Technique to Assess Ageing of MED, *37th Int. Annual Conference of ICT*, Karlsruhe, Germany, June 27–30, **2006**.

[26] S. Cerri, M. A. Bohn, K. Menke, L. Galfetti, Aging of HTPB/Al/AP Rocket Propellant Formulations Investigated by DMA Measurements, *Propellants Explos. Pyrotech.* **2013**, *38*, 190 – 198.

[27] C. Carraro, *Mise au Point d'un Lieur PU a Matrice Polyether en Phase Aqueuse*, Internship SNPE Materiaux Energetiques, ENSCCF, Clermont-Ferrand, France, **2005**.

[28] N. Desgardin, S. Chevalier, M. Grevin, *Durée de vie*, Report CRB N°12/06/CRB/DPS/CRA/DR, Centre de Recherches du Bouchet, Vert-le-Petit, France, **2006**.

[29] J. P. Foley, J. G. Dorsey, A Review of the Exponentially Modified Gaussian (EMG) Function – Evaluation and Subsequent Calculation of Universal Data, *J. Chromatogr. Sci.* **1984**, *22*, 40 – 46.

[30] M. S. Jeansonne, J. P. Foley, Review of the Exponentially Modified Gaussian (EMG) Function Since 1983, *J. Chromatogr. Sci.* **1991**, *29*, 258–266.

[31] Design Expert Software, http://www.statease.com/software.html.

[32] M. Ahsanullah, *Focus on Applied Statistics*, Nova Science Publishers, Hauppauge, **2003**.

Received: March 10, 2014
Revised: January 28, 2015
Published online: March 25, 2015

